Unprecedented Head-to-Head Right-Handed Cross-Links between the Antitumor Bis(μ- N,N ‘-di- p -tolylformamidinate) Dirhodium(II,II) Core and the Dinucleotide d(ApA) with the Adenine...

ARTICLE *in* JOURNAL OF THE AMERICAN CHEMICAL SOCIETY · NOVEMBER 2007

Impact Factor: 12.11 · DOI: 10.1021/ja073422i · Source: PubMed

J|A|C|S
ARTICLES
Published on Web 09/21/2007

Unprecedented Head-to-Head Right-Handed Cross-Links between the Antitumor Bis(*μ*-*N,N′*-di-*p*-tolylformamidinate) Dirhodium(II,II) Core and the Dinucleotide d(ApA) with the Adenine Bases in the Rare Imino Form

Helen T. Chifotides* and Kim R. Dunbar*

Contribution from the Department of Chemistry, Texas A&M University, College Station, Texas 77843

Received May 14, 2007; E-mail: chifotides@mail.chem.tamu.edu; dunbar@mail.chem.tamu.edu

Abstract: Reactions of the anticancer active compound *cis*-$[Rh_2(DTolF)_2(CH_3CN)_6](BF_4)_2$ with 9-ethyladenine (9-EtAdeH) or the dinucleotide d(ApA) proceed with bridging adenine bases in the rare imino form (A*), spanning the Rh−Rh bond at equatorial positions via N7/N6. The inflection points for the pH-dependent H2 and H8 NMR resonance curves of *cis*-$[Rh_2(DTolF)_2(9\text{-}EtAdeH)_2](BF_4)_2$ correspond to N1H deprotonation of the metal-stabilized rare imino tautomer, which takes place at $pK_a \approx 7.5$ in CD_3CN-d_3, a considerably reduced value as compared to that of the imino form of 9-EtAdeH. Similarly, coordination of the metal atoms to the N7/N6 adenine sites in $Rh_2(DTolF)_2\{d(ApA)\}$ induces formation of the rare imino tautomer of the bases with a concomitant substantial decrease in the basicity of the N1H sites ($pK_a \approx 7.0$ in CD_3CN-d_3), as compared to the imino form of the free dinucleotide. The presence of the adenine bases in the rare imino form, due to bidentate metalation of the N6/N7 sites, is further corroborated by DQF-COSY H2/N1H and ROE N1H/N6H cross-peaks in the 2D NMR spectra of $Rh_2(DTolF)_2\{d(ApA)\}$ in CD_3CN-d_3 at −38 °C. Due to the N7/N6 bridging mode of the adenine bases in $Rh_2(DTolF)_2\{d(ApA)\}$, only the anti orientation of the imino tautomer is possible. The imino form A* of adenine in DNA may result in AT→CG transversions or AT→GC transitions, which can eventually lead to lethal mutations. The HH arrangement of the bases in $Rh_2(DTolF)_2\{d(ApA)\}$ is indicated by the H8/H8 NOE cross-peaks in the 2D ROESY NMR spectrum, whereas the formamidinate bridging groups dictate the presence of one right-handed conformer HH1R in solution. Complete characterization of $Rh_2(DTolF)_2\{d(ApA)\}$ by 2D NMR spectroscopy and molecular modeling supports the presence of the HH1R conformer, anti orientation of both sugar residues about the glycosyl bonds, and N-type conformation for the 5′-A base.

Introduction

In recent years, dirhodium compounds with metal−metal bonds[1] have drawn much attention due to their considerable carcinostatic activity against various tumor cell lines,[2−9] as well as their notable interactions with DNA[10] and other molecules of biological importance.[11,12] In this respect, the compound *cis*-$Rh_2(DTolF)_2(O_2CCF_3)_2(H_2O)_2$ (Chart 1; $DTolF^-$ = anion of *N,N′*-di-*p*-tolylformamidinate), with two robust amidinate groups,[1] exhibits in vivo antitumor activity comparable to that of dirhodium carboxylates and cisplatin (when supplied in the same quantity) against Yoshida ascites and T8 sarcomas with considerably reduced toxicity.[13] The antitumor behavior of *cis*-$Rh_2(DTolF)_2(O_2CCF_3)_2(H_2O)_2$ (and other dirhodium carboxylate compounds)[10] is attributed to DNA binding and inhibition of DNA replication.[13] Despite the presence of two labile trifluoroacetate bridging groups, which impart to the complex appreciable reactivity, *cis*-$Rh_2(DTolF)_2(O_2CCF_3)_2(H_2O)_2$ was shown to be virtually nontoxic to mice.[13] Conversely, the homoleptic paddlewheel compound $Rh_2(DTolF)_4$ exhibits no appreciable biological activity presumably due to steric factors.[14]

Interest in the reactions of dirhodium compounds[10] with purine nucleobases,[15−20] nucleos(t)ides,[21,22] as well as

(1) Chifotides, H. T.; Dunbar, K. R. Rhodium Compounds. In *Multiple Bonds Between Metal Atoms*, 3rd ed.; Cotton, F. A., Murillo, C., Walton, R. A., Eds.; Springer-Science and Business Media, Inc.: New York, 2005; Chapter 12, pp 465−589.
(2) Hughes, R. G.; Bear, J. L.; Kimball, A. P. *Proc. Am. Assoc. Cancer Res.* **1972**, *13*, 120.
(3) Howard, R. A.; Kimball, A. P.; Bear, J. L. *Cancer Res.* **1979**, *39*, 2568.
(4) Erck, A.; Rainen, L.; Whileyman, J.; Chang, I.-M.; Kimball, A. P.; Bear, J. L. *Proc. Soc. Exp. Biol. Med.* **1974**, *145*, 1278.
(5) Bear, J. L.; Gray, H. B., Jr.; Rainen, L.; Chang, I. M.; Howard, R.; Serio, G.; Kimball, A. P. *Cancer Chemother. Rep.* **1975**, *59*, 611.
(6) Howard, R. A.; Sherwood, E.; Erck, A.; Kimball, A. P.; Bear, J. L. *J. Med. Chem.* **1977**, *20*, 943.
(7) Zyngier, S.; Kimura, E.; Najjar, R. *Braz. J. Med. Biol. Res.* **1989**, *22*, 397.
(8) Bear, J. L. In *Precious Metals 1985: Proceedings of the Ninth International Precious Metals Conference*; Zysk, E. D., Bonucci, J. A., Eds.; Int. Precious Metals: Allentown, PA, 1986; p 337.
(9) De Souza, A. R.; Coelho, E. P.; Zyngier, S. B. *Eur. J. Med. Chem.* **2006**, *41*, 1214.
(10) Chifotides, H. T.; Dunbar, K. R. *Acc. Chem. Res.* **2005**, *38*, 146.
(11) Sorasaenee, K.; Fu, P. K.-L.; Angeles-Boza, A. M.; Dunbar, K. R.; Turro, C. *Inorg. Chem.* **2003**, *42*, 1267.
(12) Chifotides, H. T.; Fu, P. K.-L.; Dunbar, K. R.; Turro, C. *Inorg. Chem.* **2004**, *43*, 1175.
(13) Fimiani, V.; Ainis, T.; Cavallaro, A.; Piraino, P. *J. Chemother.* **1990**, *2*, 319.
(14) Piraino, P.; Tresoldi, G.; Lo Schiavo, S. *Inorg. Chim. Acta* **1993**, *203*, 101−105.
(15) Pneumatikakis, G.; Hadjiliadis, N. *J. Chem. Soc., Dalton Trans.* **1979**, 596.
(16) Rubin, J. R.; Haromy, T. P. *Acta Crystallogr.* **1991**, *C47*, 1712−1714.

10.1021/ja073422i CCC: $37.00

Chart 1. Structure of *cis*-Rh$_2$(DTolF)$_2$(O$_2$CCF$_3$)$_2$L$_2$

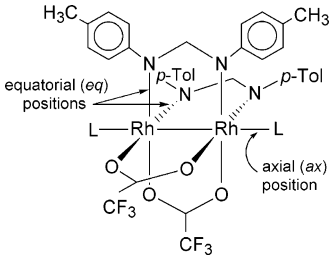

single-[23,24] and double-stranded DNA[25] stems from the fact that DNA is the primary intracellular target of most platinum-based anticancer agents.[26,27] In particular, the head-to-head 1,2-intrastrand cross-links between adjacent guanine nucleobases d(GpG) are accountable for the cell death induced by the potent anticancer agent cisplatin.[28,29] Head-to-head cross-links were also identified in the dirhodium adducts Rh$_2$(O$_2$CCH$_3$)$_2$-{d(GpG)},[21] Rh$_2$(O$_2$CCH$_3$)$_2${d(pGpG)},[22] and Rh$_2$(DTolF)$_2$-{d(GpG)}[30] with equatorial (*eq*) bidentate N7/O6 bridging guanine bases spanning the Rh−Rh bond. In the aforementioned dirhodium complexes, intense H8/H8 ROE (rotating frame nuclear Overhauser effect) cross-peaks in the 2D ROESY NMR spectra indicate HH arrangement of the tethered guanine bases. The Rh$_2$(O$_2$CCH$_3$)$_2${d(GpG)} complex exhibits two major right-handed conformers HH1R (∼75%) and HH2R (∼25%),[21] as opposed to only one right-handed HH1R conformer for Rh$_2$-(DTolF)$_2${d(GpG)}.[30] In the latter, this is most likely attributed to the presence of the bulky, non-labile formamidinate bridging groups, which slow down the possible dynamic processes for the adduct[31] and thus eliminate the formation of the minor HH2R variant observed for the acetate.[21,30] The terms HH1R and HH2R, which were coined by Kozelka et al.[32,33] and Marzilli et al.,[31,34−36] refer to the relative base canting and the direction of propagation of the phosphodiester backbone with respect to the 5′ base.[21,30] Single-stranded HH1L platinum adducts with d(GpG) appear to dominate in solution,[32,33] but HH2 variants

Chart 2. Amine and Imino Tautomeric Forms of Adenine

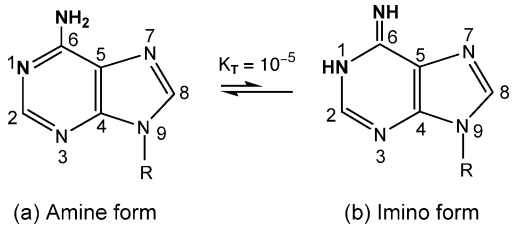

were first identified by Marzilli et al. by invoking retro models with carrier ligands on the platinum center that decrease the fluxional motion above and below the conformational plane.[31,34] The HH1R variants, however, appear to dominate in duplexes with the *cis*-Pt(NH$_3$)$_2${d(GpG)} moiety,[38] and, in this respect, the d(GpG) dirhodium HH1R variants are better models than *cis*-[Pt(NH$_3$)$_2${d(GpG)}] for the duplex DNA cross-link lesion.[31,34−36]

Adenine (Chart 2a) derivatives bind axially to dirhodium carboxylate compounds (via position N7), and the adducts are stabilized by the establishment of hydrogen bonds between the purine exocyclic NH$_2$(6) amino group and the carboxylate oxygen atom of the dirhodium unit, as evidenced by the X-ray structural studies of Rh$_2$(O$_2$CCH$_3$)$_4$(1-MeAdo)$_2$ (Ado = adenosine)[16] and *trans*-[Rh$_2$(O$_2$CCH$_3$)$_2$(HNCOCF$_3$)$_2$(9-MeAdeH$_2$)$_2$]-(NO$_3$)$_2$.[17] The reactions of *cis*-[Rh$_2$(DTolF)$_2$(CH$_3$CN)$_6$](BF$_4$)$_2$ with 9-EtAdeH, however, proceed by substitution of the acetonitrile groups and afford HT *cis*-[Rh$_2$(DTolF)$_2$(9-EtAdeH)$_2$-(CH$_3$CN)](BF$_4$)$_2$ with the adenine bases bridging via N7/N6 at *eq* sites of the two Rh centers.[39,40] This unprecedented adenine bridging binding mode in metal−metal bonded units was originally observed in the dimolybdenum analogue HT *cis*-[Mo$_2$(μ-O$_2$CCHF$_2$)$_2$(9-EtAdeH)$_2$](BF$_4$)$_2$.[41] Bidentate binding of adenine in which the base sites N7/N6 are coordinated to the same metal atom has been observed in the Ru(II) complexes [Ru(azpy)$_2$(9-MeAdeH)](PF$_6$)$_2$ and [Ru(bpy)$_2$(9-MeAdeH)]-(PF$_6$)$_2$,[42,43] in trinuclear or tetranuclear Ru(II)[44,45] and Ir(II)[46] complexes, in Pt(II)[47−49] and Pt(IV)[50] species, as well as in organometallic Mo(II),[51] Rh(III),[52] Rh(II),[53] and Rh(I)[54] complexes.

(17) Aoki, K.; Salam, Md. A. *Inorg. Chim. Acta* **2002**, *339*, 427−437.
(18) Dunbar, K. R.; Matonic, J. H.; Saharan, V. P.; Crawford, C. A.; Christou, G. *J. Am. Chem. Soc.* **1994**, *116*, 2201.
(19) Crawford, C. A.; Day, E. F.; Saharan, V. P.; Folting, K.; Huffman, J. C.; Dunbar, K. R.; Christou, G. *Chem. Commun.* **1996**, 1113.
(20) (a) Angeles-Boza, A. M.; Chifotides, H. T.; Aguirre, J. D.; Chouai, A.; Fu, P. K.-L.; Dunbar, K. R.; Turro, C. *J. Med. Chem.* **2006**, *49*, 6841. (b) Deubel, D. V.; Chifotides, H. T. *Chem. Commun.* **2007**, 3438.
(21) Chifotides, H. T.; Koshlap, K. M.; Pérez, L. M.; Dunbar, K. R. *J. Am. Chem. Soc.* **2003**, *125*, 10703.
(22) Chifotides, H. T.; Koshlap, K. M.; Pérez, L. M.; Dunbar, K. R. *J. Am. Chem. Soc.* **2003**, *125*, 10714.
(23) Chifotides, H. T.; Koomen, J. M.; Kang, M.; Tichy, S. E.; Dunbar, K. R.; Russell, D. H. *Inorg. Chem.* **2004**, *43*, 6177.
(24) Asara, J. M.; Hess, J. S.; Lozada, E.; Dunbar, K. R.; Allison, J. *J. Am. Chem. Soc.* **2000**, *122*, 8.
(25) Dunham, S. U.; Chifotides, H. T.; Mikulski, S.; Burr, A. E.; Dunbar, K. R. *Biochemistry* **2005**, *44*, 996.
(26) Zhang, C. X.; Lippard, S. J. *Curr. Opin. Chem. Biol.* **2003**, *7*, 481.
(27) Reedijk, J. *Proc. Natl. Acad. Sci. U.S.A.* **2003**, *100*, 3611.
(28) Wang, D.; Lippard, S. J. *Nat. Rev. Drug Discovery* **2005**, *4*, 307.
(29) Barnes, K. R.; Lippard, S. J. *Met. Ions Biol. Syst.* **2004**, *42*, 143−177.
(30) Chifotides, H. T.; Dunbar, K. R. *Chem.-Eur. J.* **2006**, *12*, 6458.
(31) Ano, S. O.; Intini, F. P.; Natile, G.; Marzilli, L. G. *J. Am. Chem. Soc.* **1998**, *120*, 12017.
(32) Kozelka, J.; Fouchet, M.-H.; Chottard, J.-C. *Eur. J. Biochem.* **1992**, *205*, 895.
(33) Lemaire, D.; Fouchet, M.-H.; Kozelka, J. *J. Inorg. Biochem.* **1994**, *53*, 261.
(34) Marzilli, L. G.; Ano, S. O.; Intini, F. P.; Natile, G. *J. Am. Chem. Soc.* **1999**, *121*, 9133 and references therein.
(35) Williams, K. M.; Cerasino, L.; Natile, G.; Marzilli, L. G. *J. Am. Chem. Soc.* **2000**, *122*, 8021.
(36) Sullivan, S. T.; Ciccarese, A.; Fanizzi, F. P.; Marzilli, L. G. *J. Am. Chem. Soc.* **2001**, *123*, 9345 and references therein.
(37) Bhattacharyya, D.; Marzilli, P.; Marzilli, L. G. *Inorg. Chem.* **2005**, *44*, 7644 and references therein.
(38) Yang, D.; van Boom, S. G. E.; Reedijk, J.; van Boom, J. H.; Wang, A. H.-J. *Biochemistry* **1995**, *34*, 12912.
(39) Catalan, K. V.; Hess, J. S.; Maloney, M. M.; Mindiola, D. J.; Ward, D. L.; Dunbar, K. R. *Inorg. Chem.* **1999**, *38*, 3904.
(40) Catalan, K. V.; Mindiola, D. J.; Ward, D. L.; Dunbar, K. R. *Inorg. Chem.* **1997**, *36*, 2458.
(41) Day, E. F.; Crawford, C. A.; Folting, K.; Dunbar, K. R.; Christou, G. *J. Am. Chem. Soc.* **1994**, *116*, 9339.
(42) Hotze, A. C. G.; Broekhuisen, M. E. T.; Velders, A. H.; van der Schilden, K.; Haasnoot, J. G.; Reedijk, J. *Eur. J. Inorg. Chem.* **2002**, 369.
(43) Hotze, A. C. G.; Broekhuisen, M. E. T.; Velders, A. H.; Kooijman, H.; Spek, A. L.; Haasnoot, J. G.; Reedijk, J. *J. Chem. Soc., Dalton Trans.* **2002**, 2809.
(44) Korn, S.; Sheldrick, W. S. *Inorg. Chim. Acta* **1997**, *254*, 85.
(45) Korn, S.; Sheldrick, W. S. *J. Chem. Soc., Dalton Trans.* **1997**, 2191.
(46) Annen, P.; Schildberg, S.; Sheldrick, W. S. *Inorg. Chim. Acta* **2000**, *307*, 115.
(47) Añorbe, M. G.; Lüth, M. S.; Roitzsch, M.; Cerdà, M. M.; Lax, P.; Kampf, G.; Sigel, H.; Lippert, B. *Chem.-Eur. J.* **2004**, *10*, 1046.
(48) Longato, B.; Pasquato, L.; Mucci, A.; Schenetti, L.; Zangrando, E. *Inorg. Chem.* **2003**, *42*, 7861.
(49) Longato, B.; Pasquato, L.; Mucci, A.; Schenetti, L. *Eur. J. Inorg. Chem.* **2003**, 128.
(50) Zhu, X.; Rusanov, E.; Kluge, R.; Schmidt, H.; Steinborn, D. *Inorg. Chem.* **2002**, *41*, 2667.
(51) Kuo, L. Y.; Kanatzidis, M. G.; Sabat, M.; Tipton, A. L.; Marks, T. J. *J. Am. Chem. Soc.* **1991**, *113*, 9027.
(52) Yamanari, K.; Ito, R.; Yamamoto, S.; Fuyuhiro, A. *Chem. Commun.* **2001**, 1414.
(53) Fish, R. H.; Jaouen, G. *Organometallics* **2003**, *22*, 2166.
(54) Sheldrick, W. S.; Gunther, B. *J. Organomet. Chem.* **1991**, *402*, 265.

In DNA, adenine is mainly present in its amine tautomeric form (Chart 2a),[55,56] which is estimated to exceed the rare imino form A* (Chart 2b) by a factor of 10^4-10^5. Metal binding to the exocyclic amino group N6, however, may be accompanied by a concomitant shift of the amino proton to site N1, thus generating a metalated form of the rare adenine imino tautomer.[57−59] The presence of adenine in its neutral imine form has been reported in relatively few cases of metalated adenine derivatives, for example, Ru(azpy)$_2$(9-MeAdeH-*N7*,*N6*)](PF$_6$)$_2$, [Ru(bpy)$_2$(9-MeAdeH-*N7*,*N6*)](PF$_6$)$_2$,[42,43] [(1,3-Me$_2$Uracil)Hg-(9-MeAdeH-*N6*)]NO$_3$,[60] *trans*-{[Pt(NH$_3$)$_2$(1-MeCyt-*N3*)]$_2$(9-MeAdeH-*N7*,*N6*)}(ClO$_4$)$_2$,[47] as well as in the metal−metal bonded complexes HT *cis*-[Rh$_2$(DTolF)$_2$(9-EtAdeH)$_2$(CH$_3$CN)]-(BF$_4$)$_2$[39,40] and HT *cis*-[Mo$_2$(μ-O$_2$CCHF$_2$)$_2$(9-EtAdeH)$_2$](BF$_4$)$_2$.[41] The imine form A* of adenine in DNA may result in nucleobase mispairing, due to giving rise to AT→TA,[61] AT→CG transversions, or AT→GC transitions,[58,60,62,63] which can eventually lead to mutations if not repaired. Furthermore, metal coordination to the heterocyclic rings of nucleobases may lead to unusual shifts of their pK_a values in the physiological pH range, rendering metalated nucleobases potential pH switches for biological acid−base catalysis[47,64−68] (e.g., the adenine residue in ribosomal RNA with the unusual pK_a value of 7.6 acts as a catalyst in the ribosomal peptidyl tranferase center;[69] the adenine base at the active site of a lead-dependent ribozyme has a shifted pK_a value of 6.5;[70] a protonated cytosine base acts as a catalyst for self-cleavage of the hepatitis delta virus[71]). In the case of the rare imino form of (methyl)adenine, metal coordination to N6 decreases the basicity of N1 and thus shifts the pK_a from the estimated value of 12.0[60] (for the imino tautomer) to values lower than 7.6.[47]

Armed with the knowledge from the aforementioned reports, we embarked to perform the structural characterization of the adduct formed between the biologically relevant[13] [Rh$_2$-(DTolF)$_2$]$^{2+}$ core and the {d(ApA)} dinucleotide (Chart 3) by one- (1D) and two-dimensional (2D) NMR spectroscopy along with molecular modeling studies. The NMR data as well as the pH titrations for Rh$_2$(DTolF)$_2${d(ApA)} indicate that both adenine bases are coordinated to the dirhodium core in *eq* positions via N7/N6 and are stabilized in the rare imino form due to metal binding. To our knowledge, this is the first reported bridging N7/N6 *eq* adduct between the DNA fragment d(ApA) (Chart 3) and a metal−metal bonded unit.

Chart 3. Structure and Atom Numbering of the Dinucleotide d(ApA)

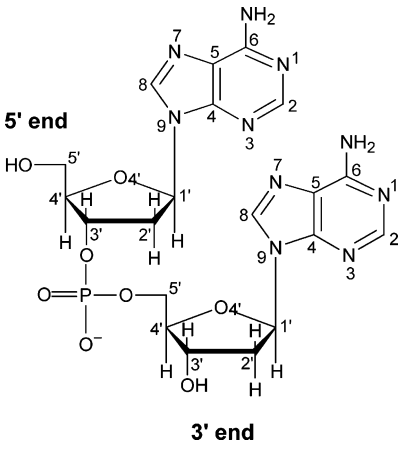

Experimental Section

Materials. The reagent 9-ethyladenine (9-EtAdeH) was purchased from Sigma. The starting material RhCl$_3$·*x*H$_2$O was obtained from Pressure Chemical Co. (Pittsburgh, PA) and was used without further purification. The complexes *cis*-[Rh$_2$(DTolF)$_2$(CH$_3$CN)$_6$](BF$_4$)$_2$ and *cis*-[Rh$_2$(DTolF)$_2$(9-EtAdeH)$_2$(CH$_3$CN)](BF$_4$)$_2$ were prepared according to literature procedures.[39] The dinucleotide d(ApA) was purchased as the crude DMT (5′-O-dimethoxytrityl) protected material from the Gene Technologies Laboratory at Texas A&M University and was purified by reverse-phase HPLC; it was used as the sodium salt. Concentrations of the dinucleotide d(ApA) were determined by UV spectroscopy at 260 nm ($\epsilon_{260} = 2.7 \times 10^4$ M^{-1} cm^{-1}). Deuterium oxide (D$_2$O, 99.996%), deuterated acetonitrile (CD$_3$CN-*d*$_3$, 99.8%), deuterium chloride (DCl, 99.5%), sodium deuteroxide (NaOD, 99.5%), and DSS (sodium 2,2-dimethyl-2-silapentane-5-sulfonate) were purchased from Cambridge Isotope Laboratories. TMP {(CH$_3$O)$_3$PO} was purchased from Aldrich.

Syntheses. (a) *cis*-[Rh$_2$(DTolF)$_2$(9-EtAdeH)$_2$(CH$_3$CN)](BF$_4$)$_2$.[39,40] A solution of 9-EtAdeH (25.1 mg, 0.154 mmol) in CH$_3$CN (6 mL) was added to a brown solution of [Rh$_2$(DTolF)$_2$(NCCH$_3$)$_6$](BF$_4$)$_2$ (82.5 mg, 0.077 mmol) in CH$_3$CN (6 mL), and the reaction solution was stirred for a few days at 37 °C. The solution gradually turned to dark green, and a green solid precipitated by addition of Et$_2$O. ESI parent ion peak {Rh$_2$(DTolF)$_2$(9-EtAdeH)$_2$ − 1}$^+$ at *m*/*z* 977.4. ^{1}H NMR (CD$_3$-CN-*d*$_3$) (δ, ppm): 10.32 (s, br, NH1), 8.08 (s, H2), 7.68 (s, H8), 7.38 (t, N−C*H*−N, $^3J\{^{103}\text{Rh}-^1\text{H}\} = 3.8$ Hz), 7.03 (m, tolyl), 6.46 (s, NH6), 4.11 (m, CH$_2$), 2.25 (s, CH$_3$(tolyl)), 1.95 (s, *ax*-CH$_3$CN), 1.25 (s, CH$_3$); free 9-EtAdeH, 8.20 (s, H2), 7.88 (s, H8), 5.95 (s, br, NH6).

(b) Rh$_2$(DTolF)$_2${d(ApA)}. In a typical reaction, [Rh$_2$(DTolF)$_2$-(NCCH$_3$)$_6$](BF$_4$)$_2$ (2.4 μmol) in 200 μL of CD$_3$CN-*d*$_3$ (brown solution) was treated with 50 μL of d(ApA) (2.4 μmol) in D$_2$O. Upon mixing the two solutions, a white precipitate formed. After the sample was incubated at 37 °C for several days, the white solid dissolved completely and the color of the solution changed from brown to olive green. The progress of the reaction was monitored by ^{1}H NMR spectroscopy until no free d(ApA) could be detected. The reaction is complete in ∼10 days. MALDI parent ion peak observed at *m*/*z* 1214 (Figure S1, Supporting Information).

Instrumentation. The 1D ^{1}H NMR spectra were recorded on a 500 MHz Varian Inova spectrometer with a 5 mm switchable probehead. The ^{1}H NMR spectra were typically recorded with 5000 Hz sweep width and 32K data points. A presaturation pulse to suppress the water peak was used when necessary. The 1D ^{13}C{^{1}H} and the Attached Proton Test[72] (^{13}C{APT}) NMR spectra were recorded on a 500 MHz Varian Inova spectrometer operating at 125.76 MHz for ^{13}C. The 1D ^{31}P NMR spectra were recorded on a Varian 300 MHz spectrometer

(55) Hanus, M.; Kabelác, M.; Rejnek, J.; Ryjácek, F.; Hobza, P. *J. Phys. Chem. B* **2004**, *108*, 2087.
(56) Laxer, A.; Major, D. T.; Gottlieb, H. E.; Fischer, B. *J. Org. Chem*. **2001**, *66*, 5463.
(57) Lippert, B. *Coord. Chem. Rev.* **2000**, *200−202*, 487.
(58) Lippert, B. *Prog. Inorg. Chem.* **2005**, *54*, 385 and references therein.
(59) Sponer, J.; Sponer, J. E.; Gorb, L.; Leszczynski, J.; Lippert, B. *J. Phys. Chem. A* **1999**, *103*, 11406.
(60) Zamora, F.; Kunsman, M.; Sabat, M.; Lippert, B. *Inorg. Chem*. **1997**, *36*, 1583.
(61) Burnouf, D.; Daune, M.; Fuchs, R. P. P. *Proc. Natl. Acad. Sci. U.S.A.* **1987**, *84*, 3758.
(62) Topal, M. D.; Fresco, J. R. *Nature* **1976**, *263*, 285.
(63) Saenger, W. *Principles of Nucleic Acid Structure*; Springer-Verlag: New York, 1984.
(64) Roitzsch, M.; Añorbe, M. G.; Miguel, P. J. S.; Müller, B.; Lippert, B. *J. Biol. Inorg. Chem.* **2005**, *10*, 800.
(65) Lüth, M. S.; Willermann, M.; Lippert, B. *Chem. Commun*. **2001**, 2058.
(66) Roitzsch, M.; Lippert, B. *J. Am. Chem. Soc*. **2004**, *126*, 2421.
(67) Pan, T.; Uhlenbeck, O. C. *Nature* **1992**, *358*, 560.
(68) Lax, P. M.; Añorbe, M. G.; Müller, B.; Bivián-Castro, E. Y.; Lippert, B. *Inorg. Chem*. **2007**, *46*, 4036.
(69) Muth, G. W.; Ortoleva-Donnelly, L.; Ströbel, S. A. *Science* **2000**, *298*, 947.
(70) Legault, P.; Pardi, A. *J. Am. Chem. Soc*. **1997**, *119*, 6621.
(71) Oyelere, A. K.; Kardon, J. R.; Ströbel, S. A. *Biochemistry* **2002**, *41*, 3667.
(72) Patt, S. L.; Shoolery, J. N. *J. Magn. Reson*. **1982**, *46*, 535.

operating at 121.43 MHz for ^{31}P. The ^1H NMR spectra were referenced to the residual proton impurity in CD_3CN-d_3, whereas the ^{13}C NMR spectra were referenced to the residual carbon impurities in CD_3CN-d_3. Trimethyl phosphate (TMP) (0 ppm) was used as an external reference for the ^{31}P NMR spectra. The 1D NMR data were processed using the Varian VNMR 6.1b software.

The 2D NMR data were collected at 10 °C on a Varian Inova 500 MHz spectrometer equipped with a triple-axis gradient penta probe. In general, the homonuclear experiments were performed with a spectral width of ~5000 Hz in both dimensions, while some high-resolution 2D [$^1H-^1H$] DQF-COSY spectra were collected with 3000 Hz spectral width. 2D [$^1H-^1H$] ROESY (rotating-frame Overhauser enhancement spectroscopy) spectra were collected with mixing times of 150 and 300 ms. A minimum of 2048 points was collected in t_2 with at least 256 points in t_1 and 32−64 scans per increment. 2D [$^1H-^1H$] DQF-COSY (double-quantum-filtered correlation spectroscopy) spectra, collected with ^{31}P decoupling in both dimensions, resulted in a 1228 × 440 data matrix with 40 scans per increment. 2D [$^1H-^{31}P$] HETCOR (heteronuclear shift correlation) experiments were collected with 2048 points in t_2, 112 points in t_1 with 512 scans per increment. The ^{31}P NMR spectral width was approximately 1500−3500 Hz. The 2D [$^1H-^{13}C$] HMBC (heteronuclear multiple bond correlation) spectrum[73] resulted from a matrix of 512 × 1024 data points with 128 acquisitions per t_1 increment. All data sets were processed using a 90° phase-shifted sine-bell apodization function and were zero filled. The baselines were corrected with first- or second-order polynomials. Two-dimensional (2D) NMR data were processed using the program nmrPipe.

The pH values of the samples were recorded on a Corning pH meter 430 equipped with a MI412 microelectrode probe by Microelectrodes, Inc. The pH values of the samples were monitored in acetonitrile/water solutions; calibration of the MI412 glass microelectrode probe was performed in standard aqueous buffer solutions. The difference in the pH of the buffer measured in an aqueous solution and its pH* in an acetonitrile/water mixture primarily depends on the liquid-junction potential of the electrode, which is negligible for the electrode used. It has been reported that, for electrodes with a negligible liquid-junction potential, the pH and pH* values for various buffers measured in aqueous and acetonitrile/water mixtures, respectively, differ by ~0.01−0.2 pH units, which is the precision expected for measurements in nonaqueous and mixed solvents.[74,75] The pH dependence of the chemical shifts for the H8 and H2 purine proton nuclei was monitored by adding trace amounts of DCl and NaOD solutions to the samples. No correction was applied to the pH values for deuterium isotope effects on the glass electrode. pH titration curves were fitted to the Henderson−Hasselbalch equation using the program KALEIDAGRAPH, with the assumption that the observed chemical shifts are weighted averages according to the populations of the protonated and deprotonated species. The $pK_{a(s)}$ values for the dirhodium adducts determined in acetonitrile/water mixtures, however, are not compared to the reported $pK_{a(w)}$ values of similar systems measured in water; they are only compared to the $pK_{a(s)}$ values of the free ligands estimated in the same acetonitrile/water solvent system. This is due to the fact that the range of the pH scale for acetonitrile (pK_a for acetonitrile = 28.5) is different from that of water.[76]

MALDI (matrix-assisted laser desorption ionization) mass spectra were acquired using an Applied Biosystems Voyager Elite XL mass spectrometer. The UV measurements were taken with a Shimadzu UV 1601PC spectrophotometer.

Molecular Modeling. Molecular modeling results were obtained using the software package Cerius^2 4.6 (Accelrys Inc., San Diego). To sample the conformational space of each compound, simulated annealing (SA) calculations in the gas phase were performed using the Open Force Field (OFF) program, with a modified version of the Universal Force Field (UFF).[77] The SA was carried out for 80.0 ps, over a temperature range of 300−500 K, with $\Delta T = 50$ K, using the Nosé temperature thermostat, a relaxation time of 0.05 ps, and a time step of 0.001 ps. The compounds were minimized (quenched) after each annealing cycle, producing 200 minimized structures. UFF is parametrized for octahedral Rh(III), whereas the molecules in the present study are metal−metal bonded Rh(II) compounds in a paddlewheel structure with axial ligands. To account for the difference in the oxidation state and the coordination environment of the metal, the valence bond parameter was modified. The valence bond parameters for these types of complexes were previously developed[21,22] and were appropriately modified for the $Rh-N_{DTolF}$ bond by taking into consideration the crystal structure of HT *cis*-$[Rh_2(DTolF)_2(9\text{-}EtAdeH)_2(CH_3CN)]^{2+}$.[39,40] The original valence bond value of 1.3320 Å for Rh(III) was set to 1.2550 Å, and all other parameters were left unmodified. The bond order for all bonds, except those including the Rh atoms, were calculated using the OFF bond order settings. The Rh−Rh and metal−ligand bond orders were set to 1.0 and 0.5, respectively. The calculated Rh−Rh bond distance obtained for the lowest energy conformer of HT *cis*-$[Rh_2(DTolF)_2(9\text{-}EtAdeH)_2]^{2+}$ is 2.50 Å.[39,40] The Rh−Rh, Rh−N6/N7(adenine), and $Rh-N_{DTolF}$ bond distances are within 0.01, 0.08, and 0.1 Å, respectively, of the crystal structure values for HT *cis*-$[Rh_2(DTolF)_2(9\text{-}EtAdeH)_2(CH_3CN)]^{2+}$.[39,40]

Results

(I) 1D ^1H NMR Spectroscopy. (a) HT *cis*-$[Rh_2(DTolF)_2(9\text{-}EtAdeH)_2(CH_3CN)](BF_4)_2$. In the aromatic region, the ^1H NMR spectrum of HT *cis*-$Rh_2(DTolF)_2(9\text{-}EtAdeH)_2(CH_3CN)](BF_4)_2$ (C_2 symmetry) in CD_3CN-d_3 displays two resonances at 8.08 (H2) and 7.68 (H8) ppm for the nonexchangeable protons, upfield from the H2 and H8 resonances of free 9-EtAdeH at 8.20 and 7.88 ppm, respectively (in CD_3CN-d_3). An upfield/downfield relationship of the H8/H2 resonances of the complex has been previously observed for N7/N6 bound adenine rings.[41,42,46,48] Characteristic upfield shifts of the nonexchangeable proton resonances of adenine have been associated with formation of the imino tautomer of the base.[78] NMR and X-ray crystallographic studies have shown that, in *cis*-$[Rh_2(DTolF)_2(9\text{-}EtAdeH)_2(CH_3CN)](BF_4)_2$, the adenine bases are present in the neutral imino form (Chart 2b).[39,40] The pH dependence study of the H2 and H8 ^1H NMR resonances of *cis*-$[Rh_2(DTolF)_2(9\text{-}EtAdeH)_2(CH_3CN)](BF_4)_2$ in CD_3CN-d_3 at 20 °C was performed to probe the behavior of the adenine base protons at various pH values (Figure 1). For the normal amino tautomer of adenine in H_2O (Chart 2a), protonation of N1 takes place at $pK_a \approx 3-4$ (which decreases to ~2 upon metal binding to N7),[51,78−81] protonation of N7 is known to occur below pH 0 (and thus is not used as a probe of N7 metal binding),[82] whereas the exocyclic group NH6 is (de)protonated at $pK_a \approx 16.7$.[83] In the case of the rare imino form of (methyl)adenine (Chart 2b),

(73) van Dongen, M. J. P.; Wijmenga, S. S.; Eritja, R.; Azorin, F.; Hilbers, C. W. *J. Biomol. NMR* **1996**, *8*, 207.
(74) Espinosa, S.; Bosch, E.; Rosés, M. *Anal. Chem.* **2000**, *72*, 5193.
(75) Espinosa, S.; Bosch, E.; Rosés, M. *J. Chromatogr., A* **2002**, *964*, 55.
(76) Mussini, T.; Covington, A. K.; Longhi, P.; Rondinini, S. *Ann. Chim.* **1983**, *73*, 675.
(77) (a) Rappé, A. K.; Casewit, C. J.; Colwell, K. S.; Goddard, W. A., III; Skiff, W. M. *J. Am. Chem. Soc.* **1992**, *114*, 10024. (b) Castonguay, L. A.; Rappé, A. K. *J. Am. Chem. Soc.* **1992**, *114*, 5832. (c) Rappé, A. K.; Colwell, K. S.; Casewit, C. J. *Inorg. Chem.* **1993**, *32*, 3438.
(78) Sowers, L. C.; Fazakerley, G. V.; Kim, H.; Dalton, L.; Goodman, M. F. *Biochemistry* **1986**, *25*, 3983.
(79) Bivián-Castro, E. Y.; Roitzsch, M.; Gupta, D.; Lippert, B. *Inorg. Chim. Acta* **2005**, *358*, 2395.
(80) Kampf, G.; Kapinos, L. E.; Griesser, R.; Lippert, B.; Sigel, H. *J. Chem. Soc., Perkin Trans.* **2002**, 1320.
(81) Peacock, A. F. A.; Parsons, S.; Sadler, P. *J. Am. Chem. Soc.* **2007**, *129*, 3348.
(82) van der Veer, J. L.; van den Elst, H.; den Hartog, J. H. J.; Fichtinger-Schepman, A. M. J.; Reedijk, J. *Inorg. Chem.* **1986**, *25*, 4657.
(83) Stuart, R.; Harris, M. G. *Can. J. Chem.* **1977**, *55*, 3807.

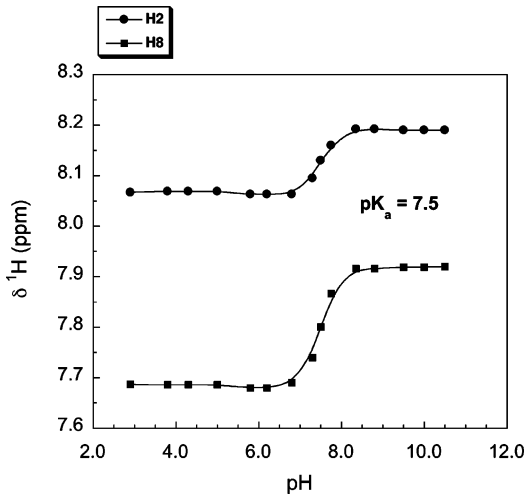

Figure 1. pH dependence of the H2 (●) and H8 (■) ^{1}H NMR resonances for HT *cis*-$Rh_2(DTolF)_2(9\text{-}EtAdeH)_2(CH_3CN)](BF_4)_2$ in CD_3CN-d_3 at 20 °C.

however, the pK_a for N1H deprotonation in H_2O has been estimated to be ∼12.[60] It is inferred that the pK_a for N1H deprotonation of the imino form of 9-EtAdeH in CD_3CN-d_3 should be considerably higher than 12.0 (i.e., the pK_a of benzylamine is 9.3 and 16.8 in H_2O and CH_3CN, respectively),[84] because it has been demonstrated that the pK_a values of neutral acids (and their conjugated bases) increase in organic solvents as compared to water (the decrease in the dielectric constant of the medium disfavors dissociation of neutral acids because it produces charged species, and thus it increases the pK_a values).[75,84] The inflection points of the curves for the H2 and H8 proton resonances of *cis*-$Rh_2(DTolF)_2(9\text{-}EtAdeH)_2(CH_3CN)](BF_4)_2$ correspond to N1H deprotonation of the imino tautomer (the two adenine bases have equivalent chemical environments and thus have overlapping deprotonation steps in the pH range studied), which takes place at p$K_a \approx 7.5$ in CD_3CN-d_3 (Figure 1), a considerably reduced value as compared to that of the imino form of 9-EtAdeH (in the same solvent). The substantial decrease in the basicity of N1H in the dirhodium complex is attributed to the presence of the rare imino tautomer of adenine, which is stabilized by binding of N6 to the dirhodium unit and subsequent protonation of site N1.

(b) $Rh_2(DTolF)_2${d(ApA)}. In the aromatic region of the ^{1}H NMR spectrum of the dirhodium adduct in CD_3CN-d_3/D_2O 80/20% at 20 °C, the four nonequivalent nonexchangeable protons of d(ApA) give rise to two sets of resonances at δ 8.84 (H8), 7.61 (H2) ppm and 7.93 (H8), 7.80 (H2) ppm, which are assigned to 5′-A and 3′-A, respectively (Figure 2; Table 1), by analysis of 2D NMR spectroscopic data (vide infra). Although the NMR data for $Rh_2(DTolF)_2${d(ApA)} and d(ApA) were collected in different solvents (the complex is not soluble in D_2O only), a comparison of the aromatic proton chemical shifts is still useful: the resonance of 5′-A H8 is downfield shifted ($\Delta\delta \approx 0.5$ ppm), the 3′-A H8 is upfield shifted ($\Delta\delta \approx 0.1$ ppm), whereas both the H2 protons are upfield shifted by $\Delta\delta \approx 0.2$ ppm, as compared to free d(ApA). Similar changes to the chemical shifts of the aromatic proton resonances of metalated adenine rings have been previously recorded in the literature,[42,44,85] and ∼0.2 ppm upfield shifts of the nonexchangeable

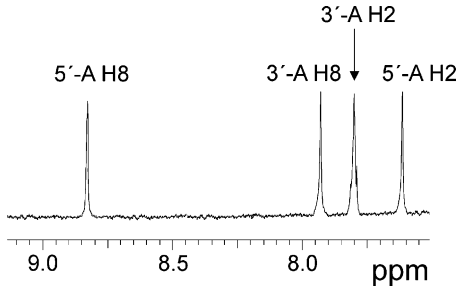

Figure 2. Aromatic region of the 1D ^{1}H NMR spectrum of $Rh_2(DTolF)_2$-{d(ApA)} in CD_3CN-d_3/D_2O 80/20% at 20 °C.

proton resonances of deoxyadenosine have been associated with formation of the imino tautomer of the base.[78] As will be inferred from the 2D NMR spectroscopic data (vide infra), the adenine bases in $Rh_2(DTolF)_2${d(ApA)} have a HH orientation (Chart 4), and it has been established from d(GpG) metalated adducts that HH orientation of the bases gives rise to disparate and downfield H8 resonances.[21,22,31,34−36] In the aromatic region, there also is a triplet at δ 7.46 ppm (with twice the intensity of each H8 or H2 resonance), which is ascribed to the two N−C*H*−N proton nuclei of the bridging formamidinate groups (the triplets are attributed to ^{1}H coupling to the two equivalent rhodium nuclei, $^3J\{^{103}Rh-^1H\} = 3.9$ Hz).

The expected pK_a value for deprotonation of the exocyclic groups NH6 of deoxyadenosine is ∼16, lower than that of methyladenine (p$K_a \approx 16.7$), due to the inductive effect of the deoxyribose group;[80,83,86] thus, the estimated pK_a value for N1H deprotonation for the imino form of deoxyadenosine in H_2O is ∼11.[60] As previously explained, the pK_a values of neutral acids (and their conjugated bases) increase in organic solvents as compared to water (vide supra); thus the estimated pK_a value-(s) for N1H deprotonation for the imino form of the d(ApA) bases in CH_3CN/H_2O should be much higher than 11.[75,84] The pH dependence curves of the 5′-A and 3′-A H2 and H8 ^{1}H NMR resonances for $Rh_2(DTolF)_2${d(ApA)} in CD_3CN-d_3/D_2O 80/20% at 20 °C are depicted in Figure 3; the inflection points of the four curves (one for each aromatic proton) at p$K_a \approx 7.0$ correspond to deprotonation of the N1H groups of the adenine bases in the rare imino form. It is inferred that the pK_a values of the NH6 sites in $Rh_2(DTolF)_2${d(ApA)} have decreased considerably as compared to the imino form of the bases in d(ApA) in the same solvent. The substantial decrease in the basicity of N1H in the bis-formamidinate dirhodium d(ApA) complex is attributed to the presence of the adenine bases in the rare imino form, which is stabilized by binding of the N7/N6 sites to the dirhodium unit.

(II) ^{13}C NMR Spectroscopy. For the aforementioned compounds, adenine binding to the dirhodium core via N6 was corroborated by means of ^{13}C NMR spectroscopy. A compendium of the ^{13}C NMR chemical shift values for 9-EtAdeH, d(ApA), and their bis-formamidinate dirhodium adducts is reported in Table 2.

For the dirhodium compounds, the assignment of the ^{13}C NMR resonances was accomplished in conjunction with the ^{13}C-

(84) Rosés, M. *J. Chromatogr., A* **2004**, *1037*, 283.
(85) Smith, D. P.; Baralt, E.; Morales, B.; Olmstead, M. M.; Maestre, M. F.; Fish, R. H. *J. Am. Chem. Soc.* **1992**, *114*, 10647.
(86) Reichelová, V.; Albertioni, F.; Liliemark, J. *J. Chromatogr., A* **1994**, *667*, 37.
(87) Prestsch, E.; Bühlmann, P.; Affolter, C. *Structure Determination of Organic Compounds*; Springer-Verlag: Berlin, 2000.

Table 1. ^{1}H and ^{31}P NMR Chemical Shifts (δ, ppm) for Rh$_2$(DTolF)$_2${d(ApA)}

d(ApA) species	A	H8	H2	H1′	$^3J_{H1'-H2'}$/ $^3J_{H1'-H2''}$[c]	H2′	H2″	H3′	H4′	H5′/H5″	N1H/ N6H[f]	base sugar	^{31}P[g]
Rh$_2$(DTolF)$_2${d(ApA)}[a]	5′	8.84	7.61	6.27	0/7.0(d)	2.13	2.63	4.78	3.96	3.78[d]	7.30/6.90	anti	−3.20
	3′	7.93	7.80	6.25	11.1/6.0(dd)	2.30	2.41	4.45	4.02	3.97[d]	10.75/6.62	anti	
d(ApA)[b]	5′	8.34	7.86	6.28		2.50	2.80	4.80[d]	4.25[d]	3.72[d]		anti	−4.14
	3′	8.00	8.06	6.10		2.18	2.50	4.80[d]	4.25[d]	4.18/4.12[e]		anti	

[a] 2D NMR spectra collected in CD_3CN-d_3/D_2O 80/20% at 10 °C. [b] 2D NMR spectra collected in D_2O at 5 °C. [c] In Hertz. [d] Overlapped resonances. [e] Not stereospecifically assigned. [f] Chemical shifts at −38 °C in CD_3CN-d_3. [g] Referenced to TMP at 0 ppm.

Chart 4. Structure and Numbering for Rh$_2$(DTolF)$_2${d(ApA)}[a]

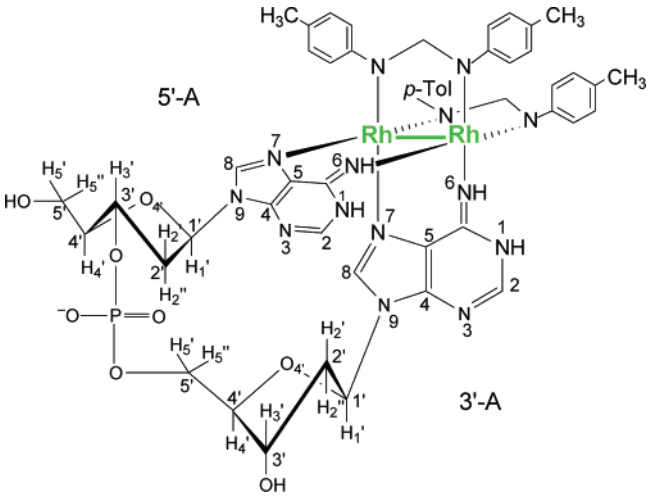

[a] Bond distances are not scaled, and angles between atoms are distorted to show structure clearly.

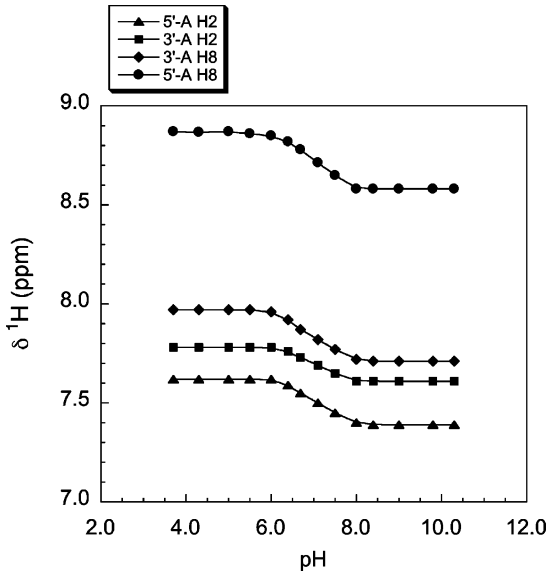

Figure 3. pH dependence of the 5′-A H2 (▲), 3′-A H2 (■), 3′-A H8 (◆), and 5′-A H8 (●) ^{1}H NMR resonances for Rh$_2$(DTolF)$_2${d(ApA)} in CD_3-CN-d_3/D_2O 80/20% at 20 °C.

{APT}[72] technique as well as by [^{1}H−^{13}C] HMBC spectroscopy[73] (vide infra). In the ^{13}C{APT} spectra, the resonances attributed to carbon atoms with an odd number of attached protons (e.g., CH and CH_3 groups) face downward, whereas the resonances of carbon atoms with an even number of attached protons (including quaternary carbon atoms) face upward.[72] The detailed assignment of the ^{13}C NMR resonances for [Rh$_2$(DTolF)$_2$(NCCH$_3$)$_6$](BF$_4$)$_2$ has been reported elsewhere.[30]

The ^{13}C NMR data for both 9-EtAdeH[56] and *cis*-[Rh$_2$(DTolF)$_2$(9-EtAdeH)$_2$(CH$_3$CN)](BF$_4$)$_2$ were collected in CD_3-CN-d_3. Although the ^{13}C NMR data for free d(ApA) were collected in a different solvent (DMSO-d_6) from the dirhodium bis-formamidinate complex, a comparison of the chemical shifts between the free ligand and the complex is still viable. For both *cis*-[Rh$_2$(DTolF)$_2$(9-EtAdeH)$_2$(CH$_3$CN)](BF$_4$)$_2$ and Rh$_2$(DTolF)$_2${d(ApA)}, the ^{13}C NMR resonances of the carbon atoms C2 and C6 are shifted upfield as compared to the free ligands (Table 2). In metalated complexes at sites N7/N6/N1, considerable downfield shifts have been observed for the ^{13}C NMR resonances of the carbon atoms C2 and C6.[49,50] Protonation of site N1 of adenine, however, results in upfield shifts of the ^{13}C NMR resonances of the carbon atoms C2 and C6.[70,88] As indicated by the pH dependence curves of the ^{13}C NMR resonances of the free nucleotides, the C2 and C6 atoms of purine rings are the most sensitive ^{13}C NMR probes for monitoring the imino protonation of site N1.[22,70] For both [Rh$_2$(DTolF)$_2$(9-EtAdeH)$_2$](BF$_4$)$_2$ and Rh$_2$(DTolF)$_2${d(ApA)}, the ^{13}C NMR data were collected at pH values below the pK_a values for N1 protonation of the imino form of the adenine bases in CD_3CN-d_3 (vide supra); thus the expected downfield shifts of the resonances for C2 and C6 for the complexes (due to metal binding) are compensated by the opposite upfield effect due to protonation of the N1H sites.[70,88] The changes $\Delta\delta$ of the chemical shifts of the ^{13}C NMR resonances for the carbons atoms that are distal to the protonation sites N1H, e.g., C4 (upfield), C5 (downfield), and C8 (downfield) of the complexes with respect to the free ligands (Table 2), are similar to other reported N7/N6 metalated adducts with adenine bases.[49,50]

(III) 2D NMR Spectroscopy. 2D ROESY, [^{1}H−^{1}H] DQF-COSY, [^{1}H−^{13}C] HMBC, and [^{1}H−^{31}P] HETCOR NMR spectra were collected to assess the structural features and assign the proton resonances of the dirhodium bis-formamidinate d(ApA) species (Table 1).

In the aromatic region of the 2D ROESY NMR spectrum of Rh$_2$(DTolF)$_2${d(ApA)}, the two H8 resonances are well separated (∼1 ppm) and exhibit intense H8/H8 NOE (nuclear Overhauser effect) cross-peaks (Figure 4), features which strongly support HH base orientation, as previously observed for bis-acetate dirhodium[21,22,30] and platinum d(GpG) compounds.[31,34−37] Head-to-tail (HT) conformers do not afford H8/H8 cross-peaks due to long H8/H8 distances.[31,34−37] The downfield H8 resonance at 8.84 ppm is unambiguously assigned to 5′-A because it exhibits a strong H8/H3′ cross-peak in the 2D ROESY spectrum, and this H3′ (4.78 ppm) has a cross-peak to the phosphodiester ^{31}P NMR resonance (−3.20 ppm) in the [^{1}H−^{31}P] HETCOR spectrum, whereas H5′/H5″−^{31}P and

(88) Barbarella, G.; Capobianco, M. L.; Tondelli, L.; Tugnoli, V. *Can. J. Chem.* **1990**, *68*, 2033.

Table 2. ^{13}C NMR Data (ppm) for 9-EtAdeH, d(ApA), and Their Dirhodium Bis-formamidinate Adducts

	purine carbon atoms					DTolF carbon atoms			
compound	C6	C2	C4	C8	C5	N–*C*H–N	4°	1°	–—CH_3
9-EtAdeH[a]	156.49	153.27	150.74	141.21	120.19				
$[Rh_2(DTolF)_2(CH_3CN)_6](BF_4)_2$[a]						169.88	135.19	129.68	20.84
							148.62	127.29	
$[Rh_2(DTolF)_2(9\text{-}EtAdeH)_2](BF_4)_2$[a,b]	153.91	152.34	145.80	143.70	123.84	169.90	148.60	129.59	20.79
							134.12	127.68	
deoxyadenosine[c]	156.10	153.25	149.05	141.18	119.70				
d(ApA)[d]	156.12	152.56	149.20	139.57	119.30				
	155.95	152.43	148.91	139.35	118.94				
$Rh_2(DTolF)_2${d(ApA)}[e]	151.30	150.15	143.92	141.54	122.90	169.00	148.65	129.94	20.91
	151.80	150.42	145.01	141.93	123.70	169.85	148.58	129.81	20.85
							135.63	127.51	
							135.10	127.62	

[a] ^{13}C NMR spectra collected in CD_3CN-d_3.[56] [b] The ^{13}C NMR resonances for the CH_3- and $-CH_2-$ groups of 9-EtAdeH appear at 15.87 and 40.76 ppm, respectively. [c] ^{13}C NMR spectra collected in D_2O.[87] [d] ^{13}C NMR spectra collected in DMSO-d_6.[88] [e] ^{13}C NMR data collected in CD_3CN-d_3/D_2O 80/20%.

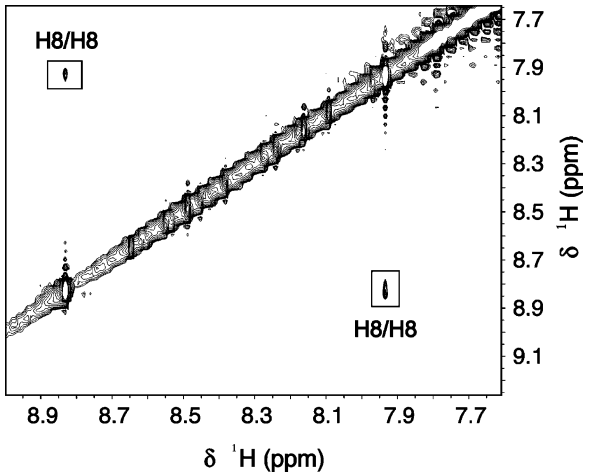

Figure 4. Aromatic region of the 2D ROESY NMR spectrum for $Rh_2(DTolF)_2${d(ApA)} in CD_3CN-d_3/D_2O 80:20% at 10 °C.

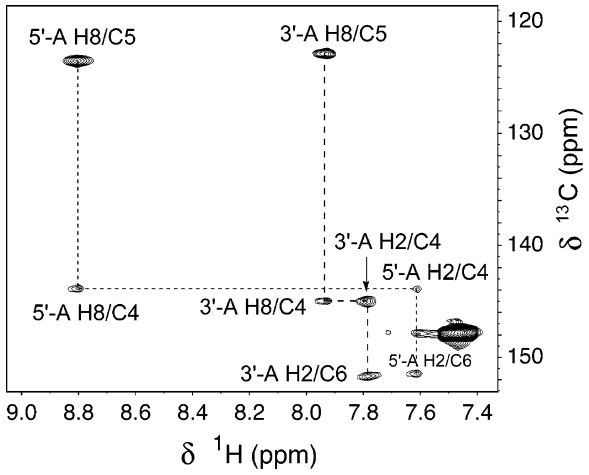

Figure 5. HMBC spectrum of $Rh_2(DTolF)_2${d(ApA)} in CD_3CN-d_3/D_2O 80/20% at 10 °C.

H4′–^{31}P cross-peaks are observed for 3′-A only.[21,22,30,34–37] The H3′ proton of 5′-A (4.78 ppm) has a much weaker cross-peak (as compared to the intraresidue peak with 8.84 ppm) with a resonance in the aromatic region at 7.93 ppm, which is assigned to the H8 of 3′-A.

In contrast to the H8 resonances, the two H2 resonances in $Rh_2(DTolF)_2${d(ApA)} do not exhibit H2/H2 NOE (nuclear Overhauser effect) cross-peaks (vide infra). The two H2 aromatic protons in $Rh_2(DTolF)_2${d(ApA)} were initially identified from the H8 protons by their long T_1 relaxation times,[89,90] and each H2 proton was unambiguously assigned to the 5′/3′-A base by performing a [^{1}H–^{13}C] HMBC (heteronuclear multiple bond correlation) experiment, which associates the H2 to the H8 proton of the same purine ring through long-range H2/C4/C6 and H8/C4/C5 correlations (through bond H2–H8 correlation is established via a common *J*-coupled carbon; Figure 5).[73] The H8 resonance at 8.84 ppm (5′-A; vide supra) exhibits cross-peaks to the ^{13}C resonances at 123.70 and 143.92 ppm, which are thus assigned to C5 and C4 of 5′-A, respectively. The ^{13}C resonance at 143.92 ppm (C4 of 5′-A) also has a cross-peak to a ^{1}H NMR resonance at 7.61 ppm (also correlated to C6 at 151.30 ppm), which is thus unequivocally assigned to H2 of 5′-A. Likewise, the H8 and H2 protons of 3′-A are correlated to C5/C4 and C4/C6, respectively, and the aromatic resonance at 7.80 ppm is assigned to H2 of 3′-A.

The 3′-A residue exhibits strong H8/H2′/H2″ ROE cross-peaks, and both sugar residues lack H8/H1′ ROE cross-peaks, which are features consistent with anti glycosidic torsion angles.[21,22,30,34–37,91] Furthermore, the 5′-A residue exhibits a strong H8/H3′ ROE cross-peak along with H1′–H2″ (no H1′–H2′ coupling; $^3J_{H1'-H2'} = 0$, Table 2) DQF-COSY cross-peaks and a doublet coupling pattern for its H1′ in the [^{1}H–^{1}H] DQF-COSY spectrum (Figure S2); these findings are characteristic of an C3′-endo (N-type) deoxyribose conformation for 5′-A.[21,22,30,34–37,91,92] Conversely, the 3′-A sugar retains the S (C2′-endo) conformation found in standard B-DNA, which is indicated by the appearance of a strong H1′–H2′ DQF COSY cross-peak along with the doublet of doublets coupling pattern observed for the H1′ resonance (Figure S2).[21,22,34–37,92]

Apart from the pH titration experiments (vide supra), the presence of the adenine rings in $Rh_2(DTolF)_2${d(ApA)} in the rare imino form was confirmed by [^{1}H–^{1}H] DQF-COSY spectroscopy at low temperatures, which has proven to be a powerful technique for assigning the H2 and N1H protons of adenine in the imino form.[42] In the low-field region of the

(89) Teletchéa, S.; Komeda, S.; Teuben, J.-M.; Elizondo-Riojas, M.-A.; Reedijk, J.; Kozelka, J. *Chem.-Eur. J.* **2006**, *12*, 3741.
(90) Admiraal, G.; Alink, M.; Altona, C.; Dijt, F. J.; van Garderen, C. J.; de Graaff, R. A. G.; Reedijk, J. *J. Am. Chem. Soc.* **1992**, *114*, 930.
(91) Kasparkova, J.; Mellish, K. J.; Qu, Y.; Brabec, V.; Farrell, N. *Biochemistry* **1996**, *35*, 16705.
(92) Rinkel, L. J.; Altona, C. *J. Biomol. Struct. Dyn.* **1987**, *4*, 621.

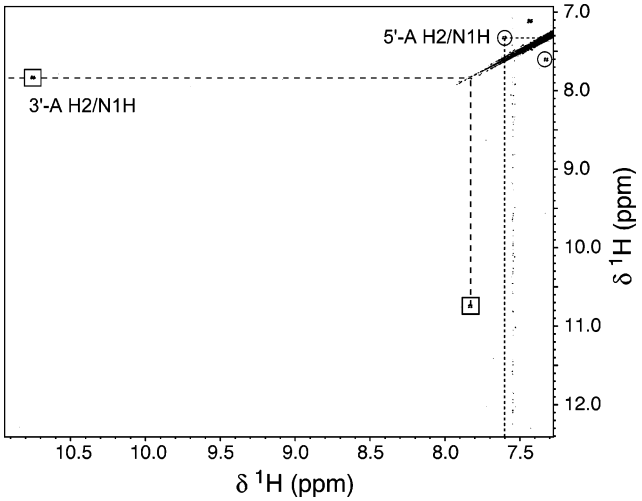

Figure 6. [^{1}H−^{1}H] DQF-COSY spectrum of $Rh_2(DTolF)_2${d(ApA)} in CD_3CN-d_3 at −38 °C. The H2/N1H cross-peaks for the 3′-A and 5′-A bases are indicated with boxes and circles, respectively.

[^{1}H−^{1}H] DQF-COSY spectrum of $Rh_2(DTolF)_2${d(ApA)} in CD_3CN-d_3 at −38 °C (Figure 6), cross-peaks (with a doublet coupling pattern) are observed between the H2 resonances of d(ApA) at 7.61 (5′-A) and 7.80 ppm (3′-A) with resonances at 7.30 (N1H 5′-A) and 10.75 ppm (N1H 3′-A), respectively, with $^3J\{^1H-^1H\} = 3$ Hz.[93] The previous H2/N1H DQF-COSY cross-peaks provide unambiguous evidence that the N1 sites of the adenine bases in $Rh_2(DTolF)_2${d(ApA)} are protonated and thus present in the rare imino form (Chart 2b), which is stabilized by the bidentate metalation of the N7/N6 sites. The upfield-shifted value for the 5′-A N1H imino proton may be attributed to the shielding effect of the tolyl group from the formamidinate bridge, as indicated by the models (vide supra). Moreover, in the ROESY spectrum of $Rh_2(DTolF)_2${d(ApA)} in CD_3CN-d_3 at −38 °C, ROE cross-peaks are observed between the 5′-A N1H (7.30 ppm) with 5′-A N6H (6.90 ppm) and the 3′-A N1H (10.75 ppm) with 3′-A N6H (6.62 ppm) resonances, further confirming protonation of the adenine N1H sites (from the X-ray crystallographic study of *cis*-[$Rh_2(DTolF)_2$(9-EtAdeH)$_2$(CH_3CN)]-(BF_4)$_2$, the adenine N1H−N6H distance is 2.25 Å[39,40]).

(IV) ^{31}P NMR Spectroscopy. The 1D ^{31}P NMR spectrum of $Rh_2(DTolF)_2${d(ApA)} in CD_3CN-d_3 displays a resonance at δ −3.20 ppm (Table 1), downfield from that of the free dinucleotide d(ApA) at δ −4.14 ppm.[21,22,30,37] Usually, the phosphate groups of HH adducts resonate ∼1 ppm downfield from the free dinucleotide. Downfield shifts of the ^{31}P NMR resonances in DNA typically indicate an increase in the unwinding angle characterized by changes in the R−O−P−OR′ torsion angles.[94]

(93) As expected, the 5′-A N1H and 3′-A N1H resonances are not observed in protic solvents; they appear as sharp ^{1}H NMR resonances in CD_3CN-d_3 at temperatures below −20 °C and split into doublets at −38 °C. Their absence from the spectra at room temperature and the broadness of these resonances at temperatures above −20 °C results from their fast exchange (on the NMR time scale) with residual water present in CD_3CN-d_3. At −38 °C in CD_3CN-d_3, both N1H resonances appear as doublets at 7.30 (5′-A) and 10.75 (3′-A) ppm, due to slower exchange of the N1H protons with residual water at low temperatures. The exchange of the N1H protons with residual water is also confirmed by the EXSY cross-peaks between residual water in CD_3CN-d_3 and the N1H protons.

(94) Gorenstein, D. G. In *Phosphorus-31 NMR*; Gorenstein, D. G., Ed.; Academic: New York, 1984.

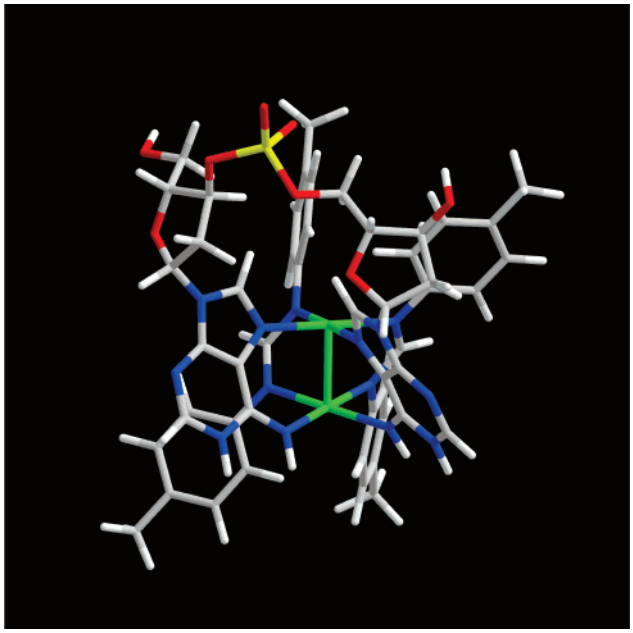

Figure 7. Lowest energy conformer, resulting from simulated annealing calculations, for the experimentally observed HH1R variant of $Rh_2(DTolF)_2$-{d(ApA)}. The 5′-A residue is positioned to the left, and 3′-A is the more canted base. Color code: Rh green, N blue, O red, P yellow, C gray, H white.

(V) Molecular Modeling. Initial HH1R, HH2R, HH1L, and HH2L conformers of the tethered adduct $Rh_2(DTolF)_2${d(ApA)} were independently constructed and subjected to simulated annealing calculations. The conformational features of the Rh_2-$(DTolF)_2${d(ApA)} adduct, suggested by the NMR data, were reproduced well by the calculations. The lowest energy HH1R variant (Figure 7) is by 2.5 kcal/mol more stable than the lowest energy HH2L variant (Table 3). The lowest energy HH1R variant is comparable in energy to the lowest energy HH1L conformer, but the HH1L and HH2R conformers were not further considered because their presence is not supported by the NMR data.

The relatively intense H8/H8 cross-peaks in the 2D ROESY NMR spectrum of $Rh_2(DTolF)_2${d(ApA)} (Figure 4) are corroborated by the H8−H8 distance in the lowest energy HH1R model (∼3.20 Å; Table 3), whereas the H2−H2 distance (∼8.90 Å) supports the absence of H2/H2 ROE cross-peaks (vide supra). In accord with the NMR data (vide supra), both the 5′-A and the 3′-A sugar residues are in the anti orientation with respect to the glycosyl bonds. The interproton H8/H3′ distance (2.35 Å) for the lowest energy HH1R conformer corroborates the strong H8/H3′ ROE NMR cross-peak(s) and thus an N-type sugar conformation for the 5′-A sugar residue. In compliance with the NMR data, 63% of the HH1R minimized models have the 3′-A deoxyribose rings in an S-type conformation. Moreover, in the model, the 5′-A N1H imino proton is in the shielding cone of the formamidinate bridge tolyl group (Figure 7), thus giving rise to an upfield-shifted resonance at 7.30 ppm (as compared to the 3′-A N1H imino proton at 10.75 ppm) in the ^{1}H NMR spectrum (vide supra). Similarly to the guanine bases in $Rh_2(O_2CCH_3)_2${d((p)GpG)},[21,22] $Rh_2(DTolF)_2${d(GpG)},[30] and *cis*-$Pt(NH_3)_2${d(pGpG)},[22] the adenine bases in the minimized HH1R $Rh_2(DTolF)_2${d(ApA)} conformer are destacked with an interbase dihedral angle 3′-A/5′-A = 73.8°.

Table 3. Summary of Lowest Energy Dirhodium Formamidinate Adducts with d(ApA) and d(GpG)

model	percent (%)[a]	energy (kcal/mol)	χ (deg)[b] 5′-B	χ (deg)[b] 3′-B	P (deg)[c] 5′-B	P (deg)[c] 3′-B	5′-B H8/ 3′-B H8 (Å)	5′-B H2/ 3′-B H2 (Å)	3′-B/5′-B dihedral angle (deg)[d]
Rh_2^2(DTolF)$_2${d(ApA)} HH1R[a]	100	297.5	−135	−163	36	163	3.20	8.90	73.8
Rh_2(DTolF)$_2${d(ApA)} HH2L	0	300.0	−2.3	−164	8	19	3.50	6.30	72.5
Rh_2(DTolF)$_2${d(GpG)} HH1R[a,e]	100	300.7	−137	−146	20	12	3.30		75.9
Rh_2(DTolF)$_2${d(GpG)} HH2L[e]	0	303.1	−1.2	−166	5	14	3.51		73.7

[a] Experimentally observed. [b] χ = O4′−C1′−N9−C4; $|\chi| > 90°$ and $|\chi| < 90°$ correspond to the anti and syn ranges, respectively, for torsion angles $-180° < \chi < +180°$. [c] P = pseudorotation phase angle calculated from the equation $\tan P = (\nu_4 + \nu_1) - (\nu_3 + \nu_0)/(\nu_2(\sin 36° + \sin 72°))$ (ν_{0-4} are endocyclic sugar torsion angles); $0° \le P \le 36°$ (±18°) corresponds to an N sugar, while $144° \le P \le 190°$ (±18°) indicates an S sugar; if $\nu_2 < 0$, $P = P + 180$. [d] Dihedral angles between 5′-B and 3′-B were calculated by using atoms N1, N3, N7 of each purine ring. [e] From ref 30.

Chart 5. Head-to-Head (HH) Variant of Rh_2(DTolF)$_2${d(ApA)} with Right (R) Canting[a]

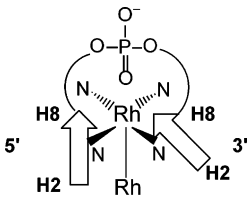

HH1R

[a] Canting arises from the fact that the adenine bases are not oriented exactly perpendicular to the N7−Rh−N7 plane. **1** refers to a model with 5′-A positioned to the left. The two rhodium atoms are depicted as face-to-face square planes with the Rh atom attached to the N7 atoms depicted on the top and the N atoms of the attached bridging formamidinate groups in the back; to show the structures clearly, the remaining coordination sites for the second Rh atom are not shown. Each A base is indicated with an arrow having H8 at the tip and H2 at the bottom. A complete description of all of the possible variants is given in ref 30.

Discussion

Conformational Features of Rh_2(DTolF)$_2${d(ApA)}. In metalated adducts with tethered bases, the dinucleotide aromatic protons are nonequivalent. The Rh_2(DTolF)$_2${d(ApA)} adduct gives rise to well-dispersed H8 proton resonances and intense H8/H8 NOE cross-peaks (Table 1), which are consistent with HH conformers. Based on the 2D NMR spectroscopic data, the downfield and upfield H8 resonances are assigned to the 5′-A and 3′-A H8 protons, respectively. In addition to the deshielding effect of the metal on both rings, each base is influenced differently by the ring-current anisotropy of the other *cis* base.[95] In compliance with the recently assessed rules for base canting,[31,34,37] 3′-A is more canted than 5′-A in Rh_2(DTolF)$_2${d(ApA)} (Chart 5) because the H8 resonance of the more canted base moves upfield due to the ring current effects of the less canted base. As expected, the H2 protons of the bases have the opposite chemical shift relationship from the H8 protons;[95,96] that is, the downfield and upfield resonances at 7.80 and 7.61 ppm are assigned to the 3′-A and 5′-A H2 protons, respectively (Table 1). Taking into consideration both the experimental evidence from the NMR spectroscopic data as well as the molecular modeling results (Table 3), the only Rh_2(DTolF)$_2${d(ApA)} conformer present in solution is assigned to the right-handed variant HH1R (Chart 5), which has precedent for acetate[21] and formamidinate[30] dirhodium d(GpG) but not for d(ApA) dinucleotide adducts. As in the case of the Rh_2(DTolF)$_2${d(GpG)} adduct,[30] most likely the bulk and the non-labile character of the formamidinate groups slows down the possible dynamic processes for Rh_2(DTolF)$_2${d(ApA)} and favors the formation of the HH1R conformer. Thus, the Rh_2(DTolF)$_2${d(ApA)} adduct gives rise to an R minihelix variant, and, in this aspect, it is a good model for the duplex DNA cisplatin cross-link lesion, because in duplexes with the *cis*-Pt(NH$_3$)$_2${d(GpG)} moiety, the HH1R variants appear to dominate.[32,33]

The 2D NMR spectroscopic data for the Rh_2(DTolF)$_2${d(ApA)} adduct support anti orientation of both sugar residues about the glycosyl bonds, retention of the 3′-A deoxyribose in the S-type (C2′-endo) conformation, whereas the 5′-A residue adopts an N-type (C3′-endo) conformation. Surprisingly, in Rh_2(DTolF)$_2${d(GpG)}, the 3′-G deoxyribose prefers the N (C3′-endo) conformation;[30] thus, in Rh_2(DTolF)$_2${d(ApA)}, most likely electronic factors of the adenine bases[63,97] are responsible for retention of an S-type 3′-A sugar ring. The aforementioned features of Rh_2(DTolF)$_2${d(ApA)} bear close resemblance to those of cisplatin dinucleotide adducts, which typically are HH cross-linked adducts with anti/anti 5′-G and 3′-G sugar residues in the N and S conformations, respectively.[98,99]

N6/N7 Bidentate Binding and Rare Imino Tautomer of the Bases. As previously reported from the X-ray crystal structure of HT *cis*-[Rh_2(DTolF)$_2$(9-EtAdeH)$_2$(CH$_3$CN)](BF$_4$)$_2$, the 9-EtAdeH bases adopt *eq* bridging interactions via atoms N7/N6 of the purine rings and span the dirhodium unit in a *cis* disposition.[39,40] Herein, the presence of the 9-EtAdeH in the complex in the rare imino form was probed by a pH dependence study of the H2 and H8 ^{1}H NMR resonances of HT *cis*-[Rh_2(DTolF)$_2$(9-EtAdeH)$_2$(CH$_3$CN)](BF$_4$)$_2$ in CD$_3$CN-d_3 at 20 °C. The H2 and H8 ^{1}H NMR resonances of HT *cis*-[Rh_2(DTolF)$_2$(9-EtAdeH)$_2$(CH$_3$CN)](BF$_4$)$_2$ shift upfield with decreasing pH (Figure 1). Formation of the rare imino tautomer of adenine has been associated with upfield shifts of the nonexchangeable proton resonances (due to a decrease of the in-plane ring current deshielding), whereas downfield shifts are diagnostic of base protonation.[78] Moreover, the pH titration exhibits only one (de)-protonation step taking place at p$K_a \approx 7.5$ in CD$_3$CN-d_3, a considerably reduced value as compared to that for N1 (de)-protonation of the imino form of free 9-EtAdeH in CD$_3$CN-d_3, which is estimated to be considerably higher than 12 in organic solvents.[60,75,84] The decrease in the basicity of N1H has been correlated to the presence of the rare imino form of adenine, due to N6/N7 bidentate metal binding.[47] Similarly, the pK_a value

(95) Marzilli, L. G.; Marzilli, P. A.; Alessio, E. *Pure Appl. Chem.* **1998**, *70*, 961.
(96) Iwamoto, M.; Alessio, E.; Marzilli, L. G. *Inorg. Chem.* **1996**, *35*, 2384.
(97) Remin, M. *J. Biomol. Struct. Dyn.* **1997**, *15*, 251.
(98) den Hartog, J. H. J.; Altona, C.; Chottard, J. C.; Girault, J. P.; Lallemand, J. Y.; de Leeuw, F. A. A. M.; Marcelis, A. T. M.; Reedijk, J. *Nucleic Acids Res.* **1982**, *10*, 4715.
(99) Mantri, Y.; Lippard, S. J.; Baik, M.-H. *J. Am. Chem. Soc.* **2007**, *129*, 5023.

Chart 6. Metal-Stabilized Syn and Anti Rare Imino Tautomers of Adenine

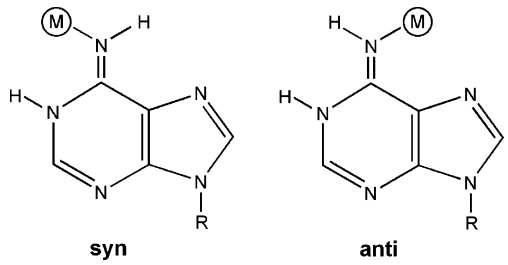

(~7.0) inferred from the pH-dependent ^{1}H NMR titration curves for the H8 and H2 resonances for both 5′-A and 3′-A of Rh_2-(DTolF)$_2${d(ApA)} in CD_3CN-d_3/D_2O 80/20% (Figure 3) is considerably reduced as compared to the free imino tautomer of d(ApA); the latter is induced by bidentate purine binding to the rhodium centers via N7/N6 and stabilization of the adenine bases in the rare imino form.[58] A pronounced acidification of N1 due to metal binding to the N7/N6 sites of adenine has been recorded in other cases (a direct comparison of the pK_a values of this study with the reported cases, however, is not appropriate due to the different solvents used in the pH titration studies); for example, for [Pt(dien)(9-MeAdeH-*N6*)]$(ClO_4)_2$ the pK_a value drops to 7.6,[58] for the chelate Ru(azpy)$_2$(9-MeAdeH-*N7*,*N6*)]-$(PF_6)_2$ to 6.5,[42] for *trans*-{[Pt$(NH_3)_2$(1-MeCyt)]$_2$(9-MeAdeH-*N7*,*N6*)}$(ClO_4)_2$ to 5.0,[47] for [(1,3-Me_2Uracil)Hg(9-MeAdeH-*N6*)]NO_3 to 4.5,[60] and for [$(NH_3)_5$Ru(Ado-*N6*)]Cl_3 to 2.5 or 4.9, depending on the syn or anti conformation of the rotamer, respectively.[58] The considerable acidification for the N1H sites of the adenine bases in HT *cis*-[Rh_2(DTolF)$_2$(9-EtAdeH)$_2$(CH_3CN)]-$(BF_4)_2$ and Rh_2(DTolF)$_2${d(ApA)} is most likely enhanced due to multiple metal ion binding,[47,58] which induces shifts of their pK_a values in the physiological pH range with obvious biological implications.

The presence of the adenine bases in the rare imino form due to bidentate metalation of the N6/N7 sites is further corroborated by the H2/N1H cross-peaks (with a doublet coupling pattern) in the [^{1}H−^{1}H] DQF-COSY spectrum of Rh_2-(DTolF)$_2${d(ApA)} in CD_3CN-d_3 at −38 °C (Figure 6) and the N1H/N6H cross-peaks in the ROESY spectrum of Rh_2(DTolF)$_2$-{d(ApA)};[42] the latter provide unambiguous evidence that the N1 sites of the adenine bases in Rh_2(DTolF)$_2${d(ApA)} are protonated below the determined pK_a value (~7.0), which is considerably reduced as compared to the imino form of the free base (vide supra). Furthermore, the downfield shifts of the C2 and C6 NMR resonances due to metalation of the adenine rings are compensated by the opposite upfield effect due to protonation of the N1H sites and support the formation of the rare imino tautomer of the bases.[70,78]

Once the metal is bound to the N6 exocyclic site of the adenine ring, it may adopt two different orientations with respect to N1, either syn or anti (Chart 6).[57,58] Examples exist for both, but in the case of the dirhodium unit, due to the bidentate N7/N6 binding, only the anti orientation is possible (Figure 7). Anti orientation of the metal at N6 and an N1 protonated site, that is, the presence of the adenine in the imine form A* in metalated DNA lesions, may result in nucleobase mispairing, by inducing AT→CG transversions or AT→GC transitions.[58−60,62,63] In the case of Rh_2(DTolF)$_2${d(ApA)}, the AT→TA transversion is not possible, despite the bases being present in the imino form, because they are in the anti orientation.[63] Recent theoretical studies have clearly demonstrated that metalation of the exocyclic amino group of adenine significantly stabilizes the protonated base by ca. 10−12 kcal/mol (as compared to the free base) and favors the mispair by ca. 5 kcal/mol (as compared to the nonmetalated one);[59] formation and stabilization of mispairs can have quite significant biological implications such as metal-induced mutations that can be lethal if not repaired.[58−60,62,63]

Conclusions

The results of the present study provide unambiguous evidence that bidentate *eq* binding takes place in the Rh_2-(DTolF)$_2${d(ApA)} adduct with the d(ApA) fragment spanning the Rh−Rh bond via N7/N6 bridges. Coordination of the metal atoms to the N7/N6 adenine sites in Rh_2(DTolF)$_2${d(ApA)} induces formation of the metal-stabilized rare imino tautomer of the bases with a concomitant substantial decrease in the basicity of the N1H sites; this is evidenced by the significant decrease of the pK_a value to ca. 7.0 (inferred from the inflection points of the pH dependence curves for the H2 and H8 proton resonances) as compared to the imino form of the free dinucleotide. The presence of the adenine bases in the rare imino form due to bidentate metalation of the N6/N7 sites is further corroborated by DQF-COSY H2/N1H cross-peaks and the ROE N1H/N6H cross-peaks in the 2D NMR spectra collected for Rh_2(DTolF)$_2${d(ApA)} in CD_3CN-d_3 at −38 °C. Due to the N7/N6 bridging mode of the dirhodium unit, only the anti orientation of each metal atom with respect to the N1H site is possible, making the imino form A* of the bases prone to AT→CG transversions or AT→GC transitions with obvious biological implications. Tethering of the adenine bases dictates the HH nature of the Rh_2(DTolF)$_2${d(ApA)} adduct, whereas the formamidinate bridging groups on the dirhodium core favor the presence of one right-handed HH1R conformer in solution in analogy to Rh_2(DTolF)$_2${d(GpG)} HH1R. Salient features of the Rh_2(DTolF)$_2${d(ApA)} conformer include anti orientation of both sugar residues about the glycosyl bonds and change to an N-type conformation for the 5′-A base; these are features that resemble some of the known platinum d(GpG) adducts. The presence of the dirhodium core and the nature of the bridging groups, however, affect the preferred DNA adducts in a distinct fashion that may impart the antitumor activity to this class of compounds.

Acknowledgment. Dr. K. M. Koshlap is acknowledged for assistance with collection of the 2D NMR data and Dr. S. K. Silber for advice on the APT ^{13}C NMR data collection. Dr. Lisa Pérez is acknowledged for assistance with the molecular modeling; the Laboratory for Molecular Simulations at Texas A&M University is acknowledged for providing software and computer time. Use of the TAMU/LBMS-Applications Laboratory (Laboratory of Biological Mass Spectroscopy) is also acknowledged. The NMR instrumentation in the Chemistry Department at Texas A&M University was funded by NSF (CHE-0077917). The NMR instrumentation in the Biomolecular NMR Laborartory at Texas A&M University was supported by a grant from the National Science Foundation (DBI-9970232) and the Texas A&M University System. K.R.D. thanks the Welch Foundation (A-1449) for financial support.

Supporting Information Available: Figure S1: MALDI MS spectrum of $Rh_2(DTolF)_2\{d(ApA)\}$. Figure S2: H1′ and H2′/H2″ region of the 2D [$^1H-^1H$] DQF-COSY NMR spectrum for $Rh_2(DTolF)_2\{d(ApA)\}$ in CD_3CN-d_3/D_2O 80:20% at 10 °C. This material is available free of charge via the Internet at http://pubs.acs.org.

JA073422I